THE PENNSYLVANIA STATE UNIVERSITY
SCHREYER HONORS COLLEGE

DEPARTMENT OF ELECTRICAL ENGINEERING

POLARIZING MAGNETO-ACTIVE ELASTOMER USING A 3D-PRINTER

MICHAEL BILYK
SPRING 2014

A thesis
submitted in partial fulfillment
of the requirements
for a baccalaureate degree
in Electrical Engineering
with honors in Electrical Engineering

Reviewed and approved* by the following:

Paris Von Lockette
Associate Professor of Mechanical Engineering
Thesis Supervisor

Sven G. Bilén
Head, School of Engineering Design, Technology, and Professional Programs,
Associate Professor of Engineering Design, Electrical Engineering, and
Aerospace Engineering
Honors Adviser

* Signatures are on file in the Schreyer Honors College.

ABSTRACT

Magneto-active elastomer is a class of material that experiences a magnetorheological effect; they bend in the presence of a magnetic field. This property can be exploited to create self-assembling structures called origami structures. A difficulty in using magneto-active elastomers in origami structures is their manufacturability. Currently, magneto-active elastomer objects are created in a mold and magnetized in large batches. This prevents the necessary scale and control over the magnetization required for origami structures. A 3D printer's ability to assign properties to three dimensional coordinates makes it a natural manufacturing solution for origami materials. In this study, an electromagnet is integrated into a 3D printer variant, called a paste extruder, to magnetize the material during the printing process. Samples were extruded and exposed to a magnetic field for increasing amounts of time while curing. Data analysis shows that there is a positive correlation between the time the electromagnet was on and the remnant magnetization of the material.

KEYWORDS: Magneto-Active Elastomers, MAE, Magnetorheological effect, 3D printing, Paste extrusion, Origami structures

TABLE OF CONTENTS

LIST OF FIGURES

LIST OF TABLES

ACKNOWLEDGMENTS

Chapter 1

Introduction

Magneto-active elastomers (MAEs) develop magnetic particle–particle and particle–field interactions when in the presence of a magnetic field [1]. This property can be exploited to create complex structures capable of being actuated using a magnetic field. An application of this material can be found in origami structures, a research area that takes inspiration from the folds of Japanese origami to create complex shapes from sheets of material. Origami structures are assembled and disassembled through folding [2]. This has a range of applications from consumer products, such as the iHome iPad case, to intravenous stents, to satellites [3, 4, 5]. MAEs can be used to create origami structures that self-assemble and disassemble through the use of an external magnetic field [2].

In a recent paper, Von Lockette [1] shows that aligned, hard magnetic material deflects the most when placed in a magnetic field, and unaligned, hard magnetic material deflects the least. The magnetic material used in the experiment reported in this thesis, barium hexaferrite, is a hard magnetic material. Von Lockette's research forms the basis of MAE's use in origami structures: aligned portions of the material deflect more than unaligned portions, causing the material to bend [1].

A student research group at The Pennsylvania State University developed a proof of concept for MAE use in origami structures by attaching permanent rare earth magnets to a silicone substrate. Using an applied magnetic field, the students were able to cause the composite to bend as seen in Figure 1 [6]. A different research group is working in parallel with this effort to use MAE instead of rare earth metals. In both cases, the researchers described their difficulty in manufacturing the structures.
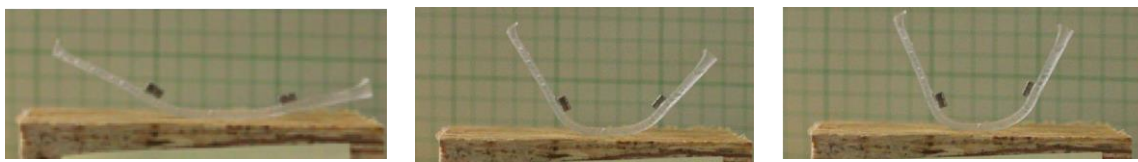
Figure 1. Rare earth magnets attached to silicone substrate, bending to varying degrees under applied magnetic field of increasing strength (left to right) [6].

A primary problem with the use of MAEs in these applications is the ability to manufacture the material at the appropriate scale and complexity. Two chief issues are the ability to create complex shapes and structures, and the ability to choose the magnetic polarization of the material at different points. Complex shapes allow for more precise structures, for instance, the material will be able to fold instead of bend—a sharp change in the vector normal to the surface, rather than a gradual change [2]. Being able to choose the polarization of the material allows for the structure to achieve multidirectional bending/folding.

Three-dimensional printers have the unique ability to attach attributes to three-dimensional coordinates and to create complex shapes. It is a natural manufacturing solution for origami materials because of these properties. Earlier laboratory work by Penn State students showed that MAE material is capable of being printed using a paste extruder, which pushes the material through a syringe. The logical next step is to determine if it is possible to polarize a portion of MAE material while printing. In this case, polarization means changing the magnetic orientation of the magnetic particles within the elastomer fluid so that they align with other particles in the area at a predictable orientation angle. If more particles are aligned, the material is more polarized and the magnetic flux density within the material, measured in tesla (T), will be higher. It is believed that there is a positive correlation between the amount of time the material is exposed to magnetic field supplied by a paste extruder while curing and the remnant magnetization of the material.

Chapter 2

Background Research

In this chapter, several topics are discussed. Included is a summary of MAE—a brief history of the material, its uses and how it works. This is followed by a description of 3D printing and how it applies to the larger problem of manufacturing origami structures. Finally, an overview of the magnetostatics that are relevant to this study is provided.

Magneto-Active Elastomers

Magneto-active elastomers are a classification of material that combines the magnetic properties of ferromagnetic particles and the elastic properties of elastomers. As the material cures, the magnetic particles become locked in place within the elastomer network. The magnetic particles activate when exposed to a magnetic field, changing the stiffness of the material. The unique properties of MAEs allow for their use in origami structures [2]. The MAE used in this study is barium hexaferrite, a hard-magnetic material, mixed with a silicone elastomer substrate. Previous works have used various elastomer compounds mixed with soft-magnetic iron particles [1].

Magneto-active elastomers have been known for some time; people have found use for them in actuation and controllable isolation devices [1]. A more novel application is the origami structures discussed earlier [2]. G. Zhou at Nanyang Technological University, as well as researchers at the University of Science and Technology of China, have determined a way to use MAEs to reduce and absorb power from the vibrations of a large structure [7, 8]. MAEs that exhibit larger than usual magnetorhelogical effect—the material stiffens more than usual when

exposed to magnetic field—have been a significant research topic since the early 2000s [1]. Recent research and development in hard-magneto-active elastomers, which exhibit rotational motion when exposed to a magnetic field, has inspired new avenues of research in recent years [9].

The magnetorheological (MR) effect describes the change in stiffness that a MAE exhibits when exposed to varying levels of magnetizing field. More specifically, it is the change in the material's complex modulus G measured in shear ΔG when placed in magnetic field **H** with respect to the complex modulus when there is no magnetic field present [1], i.e.,

$$\Delta G = \frac{G(\mathbf{H}) - G(\mathbf{H} = 0)}{G(\mathbf{H} = 0)} \ . \tag{1}$$

In soft-magnetic materials the change occurs due to magnetic particle–particle interactions producing attraction between particles; hence, the material tends to return to its undeformed shape in the presence of an external field. In hard-magnetic materials the change in stiffness (and subsequent actuation) occurs due to the torque acting upon the magnetic material within the elastomer from the external magnetic field and particle–particle interactions. When the elastomer bends, the soft-magnetic particles move creating a magnetic dipole moment, which, in conjunction with an external magnetic field, generates a torque that opposes the bend. In general, if a stronger external magnetic field is present, the stiffer the material will be. This is true up until a saturation point where increases in magnetic field strength no longer affect the stiffness of the material. In hard-magnetic particles, the magnetic dipole, **m**, exists within the particle and, hence, the torque, τ, acts directly on the particles causing bending [1].

$$\tau = \mathbf{m} \times \mathbf{B} \tag{2}$$

This material potentially could be used for intravenous or similarly small-scale devices, but MAEs are currently fabricated and magnetized in large batches, preventing the necessary scale required to build complex shapes and polarizations. An initial step towards the goal of

developing scalability in production is to develop a method for controlling the strength and

polarity of magnetization in 3D space. Three dimensional printers have the unique ability to

attach properties to a particular set of coordinates. Though previous lab work by students at Penn

State have shown MAEs can be 3D printed using a paste extruder allowing for a smaller

structural scale, limited research has been done into magnetizing the material during the printing

stage.

3D Printing

3D printing is a type of additive manufacturing process that uses extrusion to create an

object. Specifically, it is the process of taking a 3D model existing on a computer and

automatically forming it into a physical object. It works by creating machine code directions for

the printer. The directions essentially say, "Go here and perform this action." In this application,

the action can be "turn on the electromagnet for this amount of time." A 3D printer's ability to

attach attributes to specific points in a Cartesian system makes it a favorable solution for

manufacturing MAE structures. An example open-source 3D printer can be seen in Figure 2**.**

Chuck Hull invented the first 3D printer thirty years ago, in an attempt to obtain plastic

parts without waiting for tooling and molding [10]. A 3D printer lays down material, typically
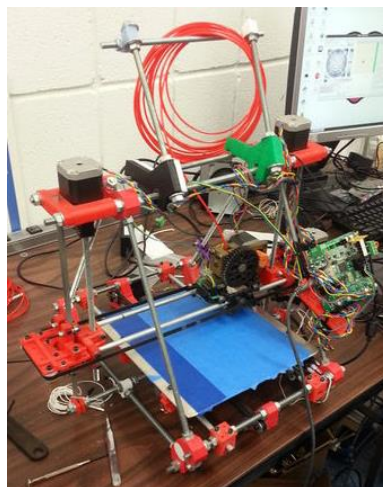
**Figure 2. A normal RepRap
OHM 3D-printer [16]**

plastic, layer by layer to build up an object as demonstrated by Figure 3. It works through fused filament fabrication, also called fused deposition modeling, in which newly extruded material fuses with previously extruded material to create a larger object, i.e., printed strands of material join together to form the object [11].

A main use of the technology is rapid prototyping because of 3D printing's ability to create unique objects more quickly and cost effectively than other methods [13]. In more recent years, the technology has become available to the general population, and is finding more use in laboratory settings. For instance, Jordan Miller at the University of Pennsylvania has been using 3D printed sugar to create blood vessel networks [14].

A paste extruder is similar to a normal RepRap 3D printer—an open source, community developed, printer—but instead of melting plastic and allowing it to harden, paste extrusion involves pushing a paste material through a syringe tip and allowing it to cure. Once the material becomes cured, another layer can be printed on top of it. In this manner, a structure made entirely of MAE can be formed without the use of a mold or tooling. For this experiment, MAE is pushed through a paste extruder onto a heated bed for curing. RepRap user "RichRap" developed the paste extruder used in this project, seen in Figure 4; it involves the use of a stepper motor to apply pressure to a syringe [15].
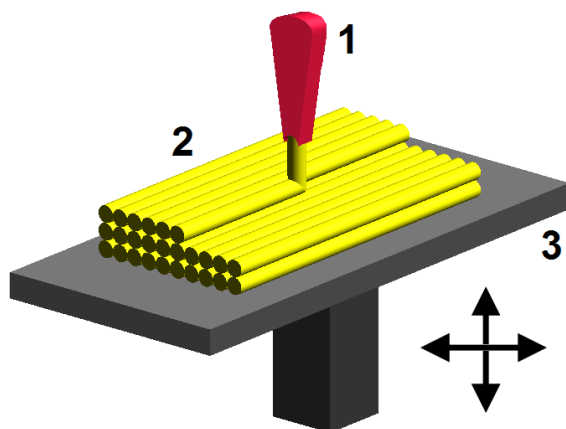
Figure 3. Material passes through the extruder tip (1), where it fused with deposited material (2) and cures on heated bed (3) [12]
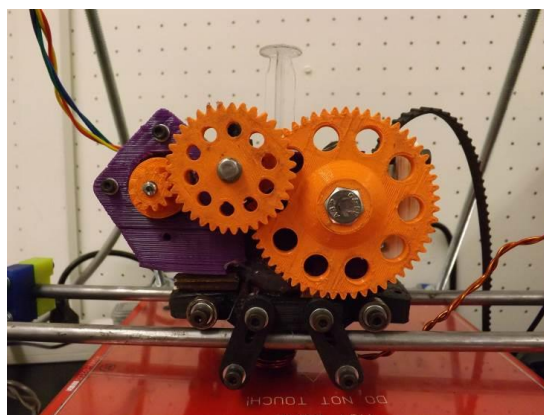
Figure 4. RepRap paste extruder without the syringe cap in place

Magnetostatics

Since MAE is a magnetic material, this experiment measures the external magnetic field as an indicator for the relative magnetization of the MAE samples. The strength of the magnetic field is determined by the relative orientation of the magnetic particles and their individual magnetic moments. The magnetic moment for each particle is a sum of the magnetic moments for the domains of the particle, which are, in turn, a sum of the magnetic moments of the atoms within those domains. A foray into some relevant elements of electromagnetics is necessary at this point.

The Biot–Savart law states that current, I, flowing in a loop with length, l, generates a magnetic field, **B**, at distance, r, with the relationship

$$\mathbf{B} = \frac{\mu_0}{4\pi} \int_C \frac{I\, d\mathbf{l} \times \mathbf{r}}{|\mathbf{r}|^2}, \tag{3}$$

where μ_0 is the permeability of free space. A magnetic moment is defined by the area of that loop and by the current present in the loop; its direction is orthogonal to the current (in accordance with right-hand rule). Magnetization in a material occurs because of the current loops at the atomic level: electrons orbiting around the nucleus and those electrons' spins as can be seen in Figure 5. Electrons orbiting and spinning are what generates magnetic field in a permanent magnet, as opposed to the magnetic field generated by electrons flowing through a wire in an electromagnet. In a ferromagnetic material, such as barium ferrite, if enough magnetic moments

(a)   (b)
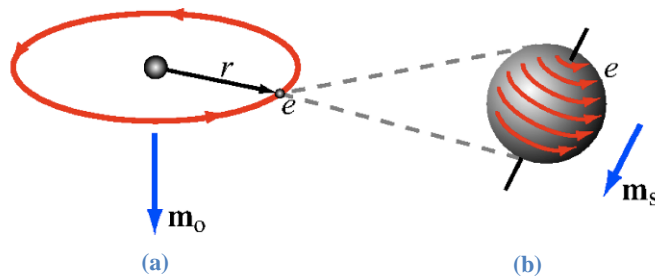
Figure 5. Magnetic moment generated from electron orbiting nucleus (a) and from the spin of the electron (b) [17]

are aligned they form a permanent magnetic domain due to strong coupling forces. The sum of the magnetization of these domains forms the overall magnetization of the material [17]. The magnetic field generated by orbiting and spinning electrons in the MAE is the magnetic field measured in this experiment.

A strong magnetic field can coerce the domains to form a dominant polarization to increase the magnetization of the particle. The magnetizing field, **H**, and magnetic field, **B**, are related through permeability, μ, by **B** = μ**H**. The permeability of ferromagnetic material is non-linear and comparing the effect of an applied magnetizing field to the magnetic B-field, one derives a magnetization curve. A large hysteresis on the magnetization curve, causing a remnant magnetization, shows that an applied magnetic field can have a permanent effect on the ferromagnetic material, and that a large amount of magnetic field, the coercive field, is required to demagnetize the material [17]. The magnetization curve of aligned and unaligned barium hexaferrite material can be seen in Figure 6. Note that, after being exposed to a large coercive magnetizing field, there is more remnant magnetization in the aligned (coerced) material than in the unaligned (un-coerced) material, parallel to the applied magnetic field [18]. In preparation for this experiment, the uncured MAE material is exposed to a large magnetic field (547 kA/m) in

(a)   (b)
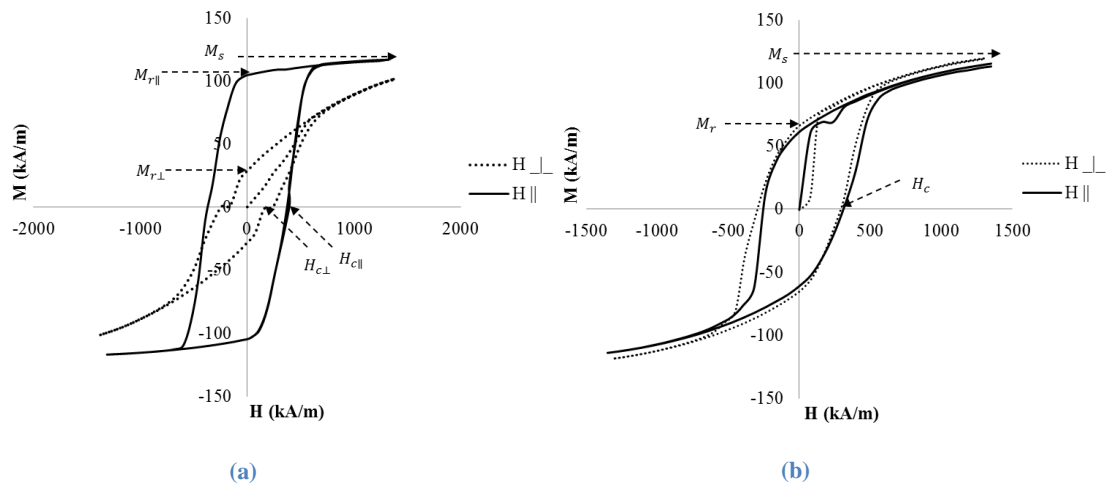
Figure 6. Magnetization curve of aligned (a) and unaligned (b) hexaferrite material [18]

order to coerce the domains of the barium hexaferrite into alignment and produce remnant

magnetization at the particle later. During the experiment, a weaker solenoid electromagnet

(4.30 kA/m) is used to align the particles in the material as it extrudes to create remnant

magnetization at the print level. At some time into the print, the magnetizing field is removed.

This experiment helps to determine the timing required to produce remnant magnetism at the

print level.

Figure 7. A Magnetech Corp. MFG-6-12 Electromagnet use a 547 kA/m magnetic field to coerce the magnet domains of the MAE into alignment to generate remnant magnetism in the MAE

Chapter 3

Experimental Methods

Summary

There are three major steps in the experimental setup: making the fluid MAE material, polarizing and printing the material, and characterizing the sample. The MAE material consists of barium hexaferrite and silicone substrate. Its magnetic domains are coerced into alignment using a high powered electromagnet. The material is placed into a syringe and extruded through a solenoid onto a heated bed where it cures for 30 minutes. The sample is removed from the print bed and placed on a sheet of graph paper. A gauss meter determines the magnetic field emanating from the cured sample. In this experiment, the amount of time the solenoid is active is varied (0 s, 1 s, 60 s, 600 s, and 1800 s) to produce different levels of remnant magnetization in MAE samples. Details of this procedure are given below.

Making the MAE

The magneto-active elastomer in this experiment is 325 mesh barium M-type hexaferrite (BaM) mixed with Sylgard 184 silicone substrate. BaM was supplied by ESPI Materials. Barium hexaferrite, with a coercive field of $\mu H_c > 0.4$ T, behaves as a hard-magnetic material. Equation 4,

$$M_{\text{BaM}} = \frac{(v/v\%_{\text{desired}})}{1-(v/v\%_{\text{desired}})} \frac{\rho_{\text{BaM}}}{\rho_{\text{SYL}}} M_{\text{SYL}}(1.1),$$

(4)

dictates the appropriate amount of each material, Catalyst is added at 10% by weight of Sylgard 184 and the solution is mixed for another five minutes. M_{BaM} is the desired mass of BaM amd M_{SYL} is the mass of the silicone used in the experiment.

The mass density for barium hexaferrite, ρ_{BaM}, and Sylgard 184 and catalyst, ρ_{SYL}, used in this experiment is 4.7 g/cm^3 and 1 g/cm^3, respectively [19]. Initial attempts to produce a 30 v/v% mixture proved too viscous to print. Consequently, a 22.6 v/v% was determined to be the highest printable concentration. After mixing, the material is transferred to a plastic zipper storage bag. The magnetic domains of the barium hexaferrite particles within the material are coerced into alignment by placing the bag in a Magnetech Corporation Magnetic Flux Generator, MFG-6-12, which consists of two powerful electromagnets in a closed magnetic loop. The spacing between the two magnets is 3/8", generating a magnetic field of 688 mT. From there, the magnetic material is mixed by kneading the bag and then transferred to a syringe.

Printing the Material

This experiment uses an Open Hybrid Mendel (OHM) model RepRap 3D-printer. The OHM printer was developed by the State College RepRap User Group near Penn State [20]. The system consists of the controller, the axis motors, the extruder, and the print bed. The printer is
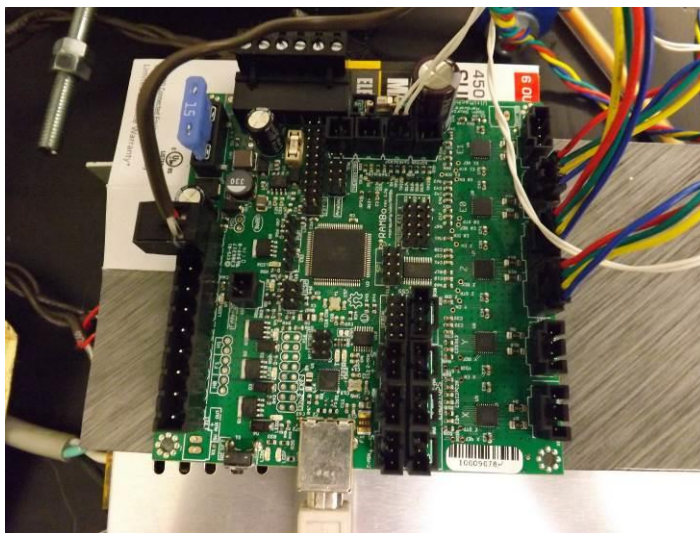
Figure 8. The RAMBo control board is used to move the axis on the 3D printer and monitor and control various other functions such as the temperature of the heated bed

controlled by a RepRap Arduino-compatible Mother Board (RAMBo) v1.2g, an electronic device

that connects to a computer and controls the printer. In this experiment, it monitors and heats the

heated print bed used for curing the MAE. In full featured paste extruders and traditional 3D

printers, the control board controls the axes system, extruder, and other printer features. The

control board was not used to control the electromagnet in this experiment but has the capability

for future setups. The device already has a built-in function for controlling the heated bed and fan

systems. These could readily be converted to control the electromagnet.

This experiment uses a paste extruder developed by RepRap user "RichRap". Although

the paste extruder's specific functions were not used in this experiment, it holds the syringe and

the solenoid. In initial tests, the paste extruder applied pressure to the syringe, but the amount and

shape of the printed material was inconsistent from sample to sample. Instead, the syringe is

actuated by hand, providing a more consistent sample size and shape.

The material is printed and cured on a PCB heated bed manufactured by MakerFarm. The

heated bed is maintained at 60 °C. At this temperature MAE takes approximately 30 minutes to

cure allowing for a shorter printing time.

The material passes through a solenoid wrapped concentrically around the syringe as

shown in Figure 9. The solenoid consists of two layers of wire with the MAE material in the
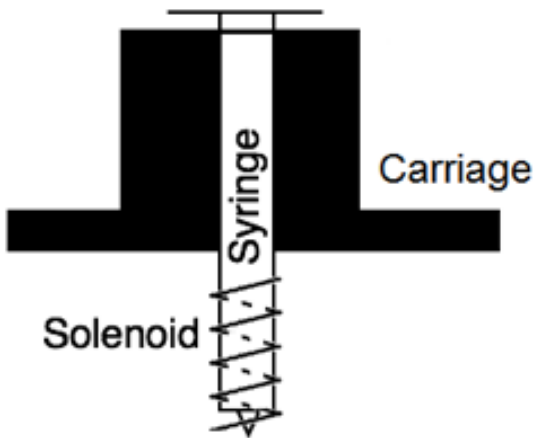
Figure 9. Solenoid placed concentrically around the syringe

Figure 10. The two layer solenoid wrapped around the syringe is glued to the bottom of the paste extruder

syringe acting as a magnetic core. Analysis showed that the remnant magnetization of the MAE

core was large enough that adding layers to the solenoid or increasing the wire gauge had little

effect on the magnetic field strength produced by the solenoid. The calculated magnetic field

from the solenoid is 100.3 kA/m and the actual magnetic field strength was 4.301 kA/m. This

discrepancy is due primarily to measuring the external field around the MAE core and not the

internal field in the MAE core. Additionally, the magnetic field from the solenoid may not have

aligned the magnetic particles in the core material, causing the effective magnetization to be

lower. Increasing the current also did not produce significant changes to the magnetic field

generated by the solenoid (see Appendix A). Regardless, there was still a desire to make the

applied magnetic field from the solenoid as powerful as possible to produce torque on the barium

ferrite particles. Therefore, two layers of wire were chosen because they fit within the extruder

carriage setup. The resistance of the wire in the solenoid coil was low enough to trip the fault

protection of the power supply. Two parallel 2-Ω 50-W resistors were added in series with the

solenoid to achieve a 1.1-Ω load. A Tenma 72-630A Regulated Power Supply provided 9 A at

10 V for 90 W of power.
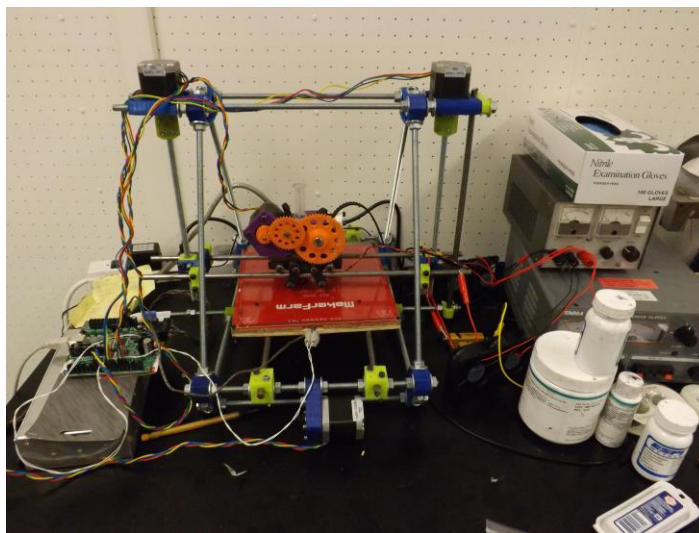
Figure 11. Experimental Setup
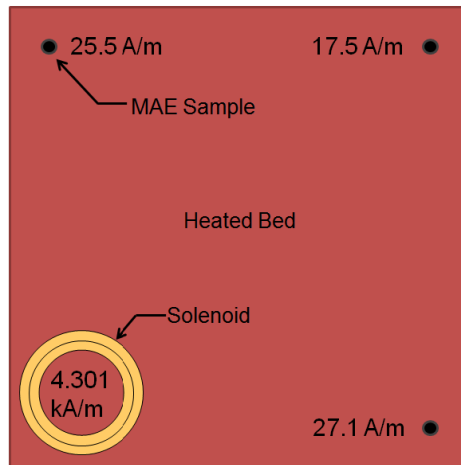
Figure 12. Staggered print samples were printed in opposite corners of the print bed to ensure that there was little effect from the solenoid while curing. The positions and their respective magnetic field strength is shown

The amount of time that the solenoid remains on while the MAE is curing is the independent variable in this experiment. The solenoid-on times are: one second, 60 seconds, 600 seconds, and 1800 seconds (the entire 30 minute cure time). There was one control group that experienced no solenoid-on time. Three samples were created for each solenoid-on time. Some solenoid-on times—one second through 600 seconds—allowed for staggering of the samples, with the next sample extruded and polled as soon as the extruder carriage became available. This saved time. The samples were printed in different corners of the heated bed to prevent effects from the solenoid. Laboratory experiments showed that the magnetic field strength at the nearest corner is 0.0255 kA/m. Compared to the 4.301 kA/m produced by the solenoid, there is a 2.2 order of magnitude difference in the magnetic field strength from the solenoid compared to the
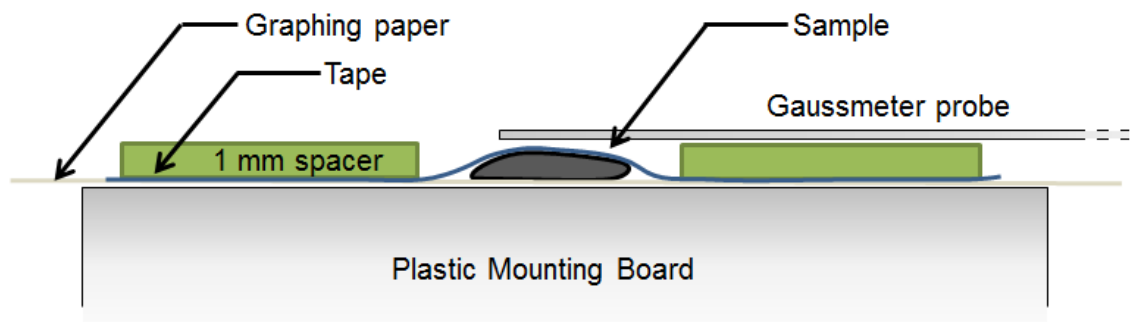
Figure 13. The mounting configuration for data collection. The material is taped onto graphing paper and placed on a mounting board. A 1mm spacer was attached to the end of the guassmeter probe used for experimentation.

magnetic field strength at the nearest corner. The dependent variable was the external magnetic field produced by the remnant magnetization of the samples normal to the carriage.

Data Collection

After printing, each sample was taped to a sheet of 1/5″ cubic graphing paper and labeled. The magnetic field is measured using a Lake Shore Model 475 DSP Gaussmeter with a ceramic probe. A one-mm spacer is placed on the end of the probe to ensure the same distance between the probe and each sample. Before measuring, the probe is calibrated on a plastic mounting board without the samples present. Next, each sample is measured five times, completely removing the probe and placing it back on the sample between each measurement. The probe was recalibrated between each sample.

Potential Issues

This research is not without its issues. Due to time constraints, magnetization was not measured directly and instead was measured through magnetic flux density. Magnetic flux density is dependent on the shape of the object and the position of the probe, and it is sensitive to the environment around it. Despite efforts to increase consistency, this remains the primary reason for the large standard deviations found in the research data.

Chapter 4

Results and Analysis

The experimental results are and are summarized in Figure 14 (full results are provided in Table 1 in Appendix B). In Figure 14, the dependent variable is the average measured external magnetic flux density in milliteslas for each sample produced. The columns represent each sample and the last column is the average magnetization of samples as a whole. The bars represent the standard deviation of the data. The standard deviation is, on average, is 59.1% of the magnetic flux density of the sample.
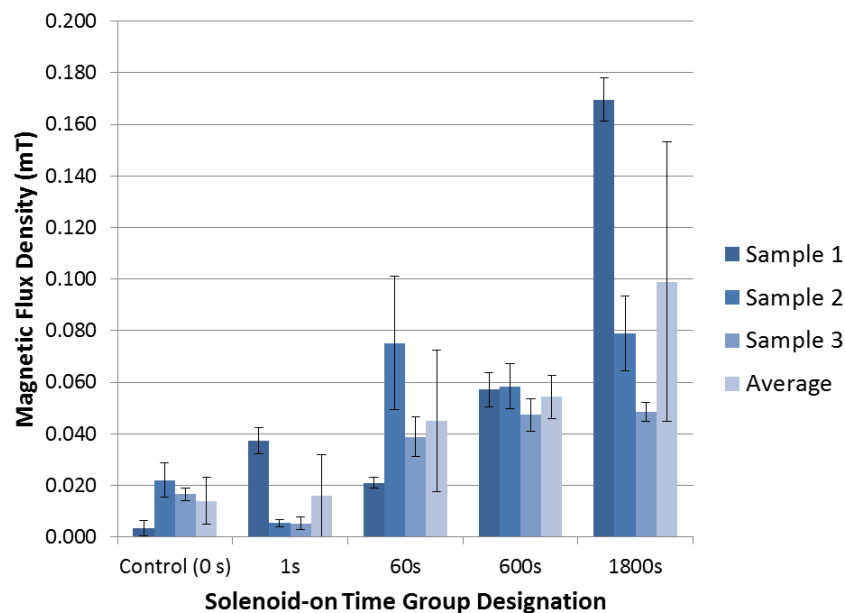
Figure 14. This graph shows the magnetic flux density of each sample and the average magnetic flux density of the group at each solenoid-on time. The black bars represent the standard deviation of data set.
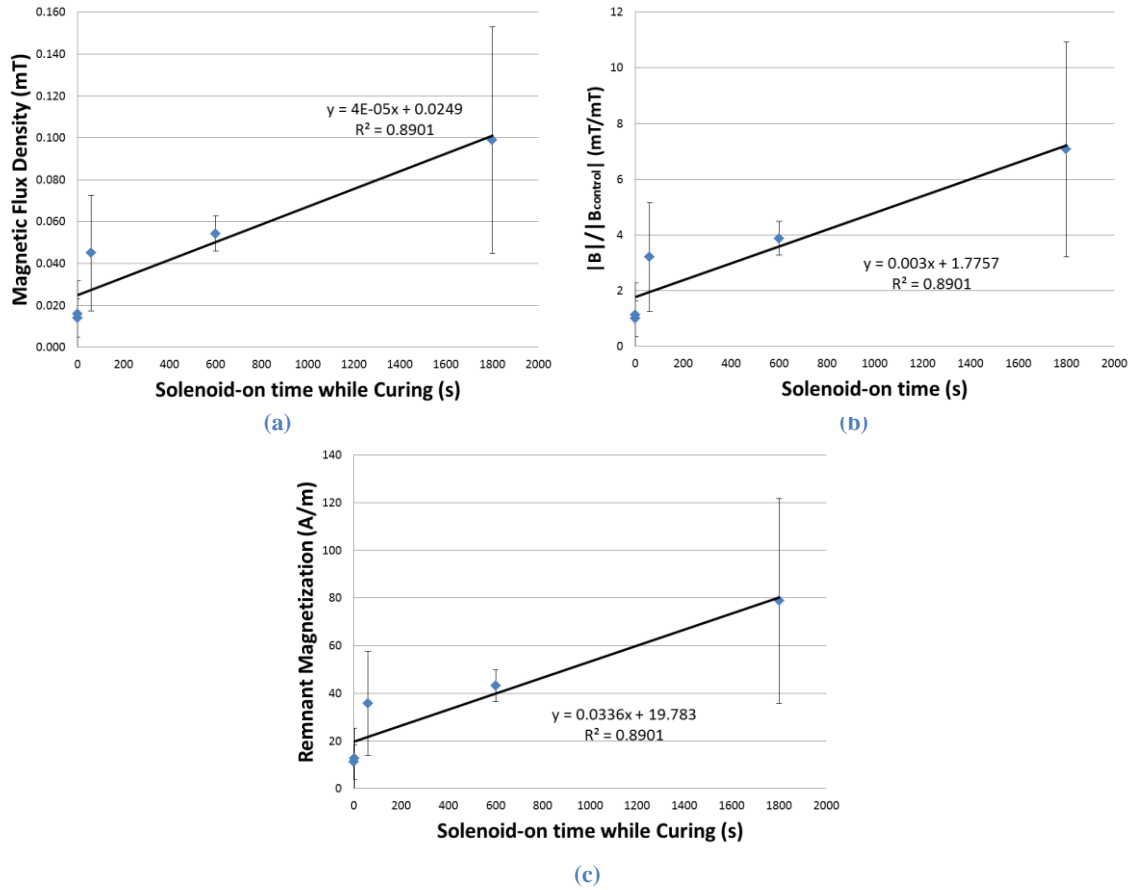
Figure 15.
(a) The average magnetic flux density of a barium hexaferrite/silicone elastomer magneto-active elastomer after being exposed to a solenoid for different periods of time while curing after being 3D printed with a paste extruder.
(b) The ratio of the average magnetic flux density for each solenoid-on time to the average magnetic flux density of the control group versus the time the solenoid was on during curing.
(c)The average remnant magnetization as a function of exposure time to a magnetic field while curing

The average magnetic flux density of each sample is plotted against the time that the solenoid was on during curing in Figure 15 (a). The independent variable is the amount of time the solenoid surrounding the syringe was active, measured in seconds. The dependent variable is the average magnetic flux density of the samples at each time period. Using the relationship between magnetic field strength and magnetic flux density ($\mathbf{B} = \mu\mathbf{H}$), the remnant magnetization strength of the material can be found, Figure 15 (c). Figure 15 (b) shows the ratio of the average magnetic flux density for each solenoid-on time to the average magnetic flux density of the control group versus the time the solenoid was on during curing.

In Figure 15 (a) a linear fit determines correlation. The equation for the linear fit is

$$|\mathbf{B}| = 4\times10^{-5}\,(\text{mT/s})\cdot t + 0.0249\,(\text{mT}), \qquad (5)$$

which has a correlation factor of $R^2 = 0.89$. The slope is the magnetization rate and the offset represents the remnant magnetization in a non-polarized region of a print. The positive slope and high correlation factor show that there is a strong correlation between the amount of time the solenoid is active while curing and the external magnetic flux density of the printed MAE. Figure 15 (b) shows that there is a 0.85 order of magnitude change in external magnetic flux density between a non-polarized MAE sample and a sample that was exposed to the solenoid for its entire curing time.

Chapter 5

Discussion

The positive correlation found between the amount of time the solenoid was on and the magnetic flux density of the exposed material shows that this prediction is correct (Figure 15 (c)). The amount of time the material is exposed to a magnetic field supplied by a paste extruder while curing has a positive effect on the magnetic flux density of the material. This relationship will only work up until a certain amount of time. Once the material cures, whether or not the electromagnet is on will have no effect on the magnetization. The trend seems to be still increasing at 1800 seconds, which could mean that material has not finished curing. DOW Corning Chemicals, the manufacturers of Sylgard 184, suggests 35 minutes of cure time at 100 °C and 2 for just the silicone elastomer [21]. Assuming linear, the curing time at 60 °C is 66 minutes. Projecting the trend using Equation **Error! Reference source not found.** gives a magnetic flux density estimate of 0.183 mT and magnetic field strength of 0.145 kA/m after 66 minutes. Regardless, this research shows it is possible to polarize the magnetic material using a 3D paste extruder.

Although it is known that aligned hard magnetic material bends more than unaligned hard magnetic material, the amount of magnetization of the material necessary to initiate MAE bending is unknown. In other experiments, the magnetic distinction between aligned and unaligned hard MAE is avoided by curing the material in extremely strong magnetic fields (>0.5 T). The amount of magnetization that this particular setup provides is low compared to what is necessary for MAE bending. As an example, in another experiment in which the researcher measured the magnetic work done by a MAE cantilever in increasing applied magnetic

fields, the remnant magnetization of the aligned hard magnet material was 103 kA/m. This is extremely high compared to the 0.0788 kA/m average remnant magnetization of the 1800 second group.

The relatively low magnetization values of the samples suggest that this more research must be done before it is ready to be used in the applications outlined earlier. With this research there is proof that a 3D printer can magnetize MAE material. If the magnetization of the material can be increased, the future could very well see 3D printing as the primary way of manufacturing MAE origami structures.

Future Research

This research involved printing a point, which is a non-dimensional shape. The next logical step towards full 3D printing capabilities is a line. Learning what happens when a varying magnetic field is applied to a line of hard MAE is a critical task to full printing capabilities. As dimensions are added, more research needs to be done on the effect of the magnetization from parts of the print on different parts of the print. Software that breaks up the 3D shape into machine code directions already exists. This software can be adapted to automatically create the machine code directions to polarize the material for origami structures. With proper development, the program could even account for the effects of magnetization from other sections of the print.

In its current setup, the printer can only polarize material in the z direction. A fully functioning MAE printer would be able to align the magnetic particles in any direction. Another avenue of future development is research methods for 3D polarization of MAE.

What magnetization is necessary for the bending characteristics required in origami structures? Answering this question will allow future developers to optimize the electromagnet timing for faster printing.

In addition to the new avenues of research this project opens up, it also provided some lessons for future iterations.

Recommendations for Future Designs

A drawback of heating the print bed is that the tip of the extruder is heated as well. The print bed is heated to 60 °C where it takes 30 minutes for the MAE material to cure. Coupled with the heat from the solenoid, the MAE material at the bottom of the syringe cures in the same way.

To solve the fast curing problem, the solenoid must move away from the syringe. A possible solution to moving the electromagnet can be found in a technique called dual extrusion. On a traditional 3D printer, dual extrusion refers to the use of two print heads to print two different materials, often colors or support structure. In this application, the second extruder could be replaced with an electromagnet, which could hover over an already extruded section to polarize the material. Decoupling the syringe and the electromagnet allows for the use of a stronger magnetic core to be used in the electromagnet. A second option to solve the fast curing of the MAE material in the syringe is to move the syringe away from the heated bed while printing.

When attempting to create a line, leakage flux will become a problem. Material polled earlier in the print will be subjected to leakage magnetic field from the solenoid. Instead, a c-shaped electromagnet can reduce leakage and create a more uniform field. This presents its own problems because the OHM printer is not designed in a way that allows for clearing for the c-shaped magnet below the print bed. An alternative 3D printer design will have to be created to accommodate the magnet.

There is still a long way to go before this technology is in ready use for MAE material, but it also is an exciting and novel technology that has a lot of room for improvement.

Chapter 6

Conclusion

This research gives insight into the timing required to polarize MAEs during paste extrusion and acts as proof-of-concept for the technology. The setup behaved as predicted and Figure 15 shows a positive correlation value of $R^2 = 0.89$ between the remnant magnetization level and magnetic field exposure time while curing. There is a 700% increase in magnetization from the samples that had no exposure to magnetic field from the solenoid and the samples that were exposed for 1800 seconds. In spite of this, the remnant magnetization levels generated in the MAE with this design are not strong enough for current MAE applications.

The result of this research helps to solve the primary problem of manufacturing MAEs. It is difficult to manufacture MAE structures quickly, cleanly, and without error. 3D printing may reduce the time of the print, reduce researcher's exposure to the material and reduce the randomness of hand manufacturing.

With work, this technology may allow for more remnant magnetization and better print resolution. With these capabilities, the 3D printer will be an invaluable tool for origami structure development. Having control of shape and polarization will allow for many new applications and will allow the realiztion of some old ones, such as the origami stents.

Despite the poor magnetization from this setup, these results prove that 3D printing technology can be used to polarize MAE during manufactuing well beyond as-mixed materials.

Appendix A

Electromagnet Wire Analysis

The correct gauge for the wire was determined through wire analysis. Figure 16 shows that there is little effect from the number layers and the gauge of the wire on the magnetic field produced by the electromagnet due to the MAE core. Ultimately, the wire gauge was chosen based availability, and the number of layers was chosen constraints on the extruder carriage. A solenoid was created using two layers and 16-AWG wire. The magnetic field strength, **H,** equals the number of layers, N, current, I, and the number of turns per inch, κ, plus the remnant magnetization, **M**$_r$. The calculated magnetic field strength of this solenoid is 100.3 kA/m. The actual magnetic field strength from this solenoid is 4.301 kA/m. This discrepancy is due primarily to measuring the external field around the MAE core and not the internal field in the MAE core. Additionally, the magnetic field from the solenoid may not have aligned the magnetic particles in the core material, causing the effective magnetization to be lower.
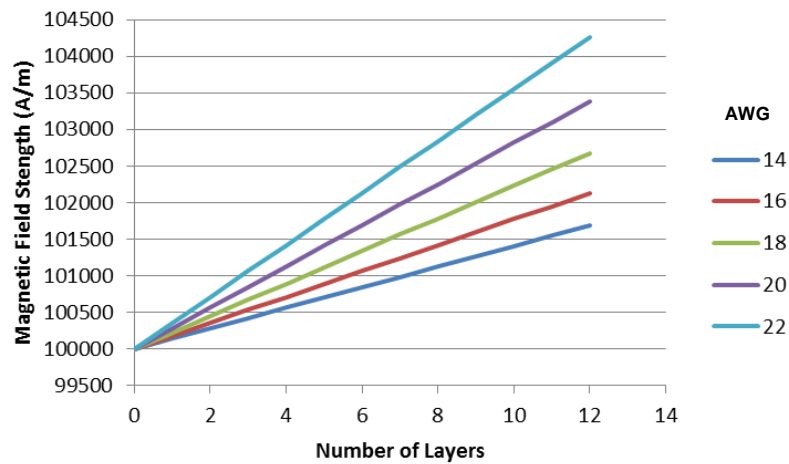
$$|\mathbf{H}| = NI\kappa + |\mathbf{M}_r| \tag{6}$$

Figure 16. Magnetic Field Strength vs Number of Layers using different Wire Gauges (AWG) at 9A

Appendix B

Experimental Data

Table 1. Experimental results. Each table represents a different solenoid-on time period

Control (0 s)	Sample		
Measure	1	2	3
Ambient	0.007 mT	0.004 mT	0.007 mT
1	0.002 mT	0.014 mT	0.016 mT
2	0.000 mT	0.017 mT	0.019 mT
3	0.008 mT	0.022 mT	0.019 mT
4	0.004 mT	0.030 mT	0.016 mT
5	0.003 mT	0.027 mT	0.013 mT
Mean	0.003 mT	0.022 mT	0.017 mT
Standard Dev	0.003 mT	0.007 mT	0.003 mT
TOTAL AVERAGE	0.014 mT		
TOTAL STANDARD DEV	0.009 mT		

1 second	Sample		
Measure	1	2	3
Ambient	0.001 mT	0.004 mT	0.000 mT
1	0.033 mT	0.006 mT	0.003 mT
2	0.032 mT	0.006 mT	0.009 mT
3	0.037 mT	0.006 mT	0.003 mT
4	0.042 mT	0.006 mT	0.006 mT
5	0.043 mT	0.003 mT	0.005 mT
Mean	0.037 mT	0.005 mT	0.005 mT
Standard Dev	0.005 mT	0.001 mT	0.002 mT
TOTAL AVERAGE	0.016 mT		
TOTAL STANDARD DEV	0.016 mT		

60 seconds	Sample		
Measure	1	2	3
Ambient	0.004 mT	0.004 mT	0.005 mT
1	0.021 mT	0.039 mT	0.045 mT
2	0.019 mT	0.072 mT	0.034 mT
3	0.019 mT	0.088 mT	0.034 mT
4	0.024 mT	0.068 mT	0.049 mT
5	0.022 mT	0.109 mT	0.032 mT
Mean	0.021 mT	0.075 mT	0.039 mT
Standard Dev	0.002 mT	0.026 mT	0.008 mT
TOTAL AVERAGE	0.045 mT		
TOTAL STANDARD DEV	0.027 mT		

600 seconds	Sample		
Measure	1	2	3
Ambient	0.006 mT	0.012 mT	0.001 mT
1	0.065 mT	0.049 mT	0.037 mT
2	0.051 mT	0.053 mT	0.049 mT
3	0.050 mT	0.060 mT	0.054 mT
4	0.062 mT	0.058 mT	0.048 mT
5	0.058 mT	0.072 mT	0.049 mT
Mean	0.057 mT	0.058 mT	0.047 mT
Standard Dev	0.007 mT	0.009 mT	0.006 mT
TOTAL AVERAGE	0.054 mT		
TOTAL STANDARD DEV	0.008 mT		

1800 seconds	Sample		
Measure	1	2	3
Ambient	0.008 mT	0.003 mT	0.002 mT
1	0.176 mT	0.071 mT	0.043 mT
2	0.179 mT	0.103 mT	0.050 mT
3	0.160 mT	0.068 mT	0.049 mT
4	0.162 mT	0.071 mT	0.047 mT
5	0.171 mT	0.082 mT	0.053 mT
Mean	0.170 mT	0.079 mT	0.048 mT
Standard Dev	0.008 mT	0.014 mT	0.004 mT
TOTAL AVERAGE	0.099 mT		
TOTAL STANDARD DEV	0.054 mT		

Bibliography

1. Von Lockette, P., S. E. Lofland, J. Biggs, J. Roche, J. Mineroff, and M. Babcock. "Investigating New Symmetry Classes in Magnetorheological Elastomers: Cantilever Bending Behavior." *Smart Materials and Structures* 20.10 (2011): 1-10. *IOP Science*. Web. 13 Jan. 2014. <http://iopscience.iop.org/0964-1726/20/10/105022/>.

2. Ahmed, Saad, Carlye Lauff, Rebecca Strzelec, Adrienne Crivaro, Kevin McGough, Robert Sheridan, Mary Frecker, Paris Von Lockette, Zoubeida Ounaies, Timothy Simpson, and Jyh-Ming Lien. "Multi-Field Responsive Origami Structures: Preliminary Modeling And Experiments." *Proceedings of the ASME 2013 International Design Engineering Technical Conferences & Computers and Information in Engineering Conference* 6B (2013): n. pag. *ASME Digital Collection*. Web. 30 Mar. 2014.

3. "Vertical Origami - Folio Cases." *Ihomecases*. IHome, n.d. Web. 01 Apr. 2014.

4. Kuribayashi, Kaori, Koichi Tsuchiya, Zhong You, Dacian Tomus, Minoru Umemoto, Takahiro Ito, and Masahiro Sasaki. "Self-deployable Origami Stent Grafts as a Biomedical Application of Ni-rich TiNi Shape Memory Alloy Foil." *Materials Science and Engineering: A* 419.1-2 (2006): 131-37. Print.

5. Monk, Meg. "BYU Engineers Use Origami to Make More Space in Space." *U N I V E R S E*. Bringham Young University, 12 Dec. 2013. Web. 01 Apr. 2014.

6. Matthews, Garrett, Nathaniel Matsuura, Melissa Martin, and Dandan She. *PSU Origami*. University Park: Pennsylvania State University, 13 Dec. 2014. PDF.

7. Zhou, G. Y. "Shear Properties of a Magnetorheological Elastomer." *Smart Materials and Structures* 12.1 (2003): 139-46. Print.

8. Deng, Hua-Xia, Xing-Long Gong, and Lian-Hua Wang. "Development of an Adaptive Tuned Vibration Absorber with Magnetorheological Elastomer." *Smart Materials and Structures* 15.5 (2006): N111-116. Print.

9. Koo, J.-H., A. Dawson, and H.-J. Jung. "Characterization of Actuation Properties of Magnetorheological Elastomers with Embedded Hard Magnetic Particles." *Journal of Intelligent Material Systems and Structures* 23.9 (2012): 1049-054. Print.

10. Hull, Chuck. "On Stereolithography." *Virtual and Physical Prototyping* 7.3 (2012): 177. Print.

11. Cary, David, Sebastien Bailard, Rene Mueller, Jasper, Matt Moses, and Glenn. "Fused Filament Fabrication." *RepRapWiki*. RepRap, 14 Jan. 2014. Web. 30 Mar. 2014.

12. Zureks. *FDM by Zureks*. Digital image. *File:FDM by Zureks.png*. Wikipedia, 2008. Web. 30 Mar. 2014.

13. Gibson, I., D. W. Rosen, and B. Stucker. *Additive Manufacturing Technologies: Rapid Prototyping to Direct Digital Manufacturing*. New York: Springer, 2010. Print.

14. Avril, Tom. "At Penn Lab, Scientists Take First Steps toward Building Human Organs." *Philly.com*. The Inquirer, 29 July 2012. Web. 30 Mar. 2014.

15. RichRap. "Universal Paste Extruder for 3D Printers." *Thingiverse*. Makerbot, 6 Apr. 2012. Web. 01 Apr. 2014. <http://www.thingiverse.com/thing:20733>.

16. "PSU Big Red Printer." *RepRapWiki*. RepRap, n.d. Web. 03 Apr. 2014.

17. Ulaby, Fawwaz T. *Fundamentals of Applied Electromagnetics*. 6e ed. Upper Saddle River, NJ: Pearson/Prentice Hall, 2010. Print.

18. Von Lockette, Paris. *Fabrication and Validation of Four Magnetic Symmetries in Magneto Active Elastomers*. N.p.: On Going Research, 4 Apr. 2014. Word Document.

19. Okazaki, Chisato, Saburo Mori, and Fumikazu Kanamaru. "Magnetic and Crystallographical Properties of Hexagonal Barium Mono-Ferrite, BaO·FeO." *Journal of the Physical Society of Japan* 16.1 (1961): 119. Print.

20. Many Authors. "Open Hybrid Mendel." *RepRapWiki*. RepRap, n.d. Web. 03 Apr. 2014. <http://reprap.org/wiki/Ohm>.

21. "Typical Properties." *Sylgard® 184 Silicone Elastomer Kit*. Dow Corning, 2014. Web. 04 Apr. 2014.

ACADEMIC VITA

Michael Bilyk
314 E. Mt. Airy Avenue
Philadelphia, PA 19119
(215) 221-2524
mvb5143@psu.edu

_____

Education

The Pennsylvania State University
University Park, PA
Schreyer Honors College
Bachelor of Science, Electrical Engineering (expected graduation May 2014)
Engineering Design Certificate Candidate

Honors and Awards

Dean's List at Pennsylvania State University,
Schreyer Honors College,
Eta Kappa Nu (Electrical Engineering Honors Society)

Association Memberships/Activities

Eta Kappa Nu (Electrical Engineering Honors Society)
IEEE
3D Printing Club

Academic Experience

Device for Community Health Workers in Kenya

Developed a medium fidelity prototype for a handheld device to aid in gathering health
data for a humanitarian venture

Comm. System for First Responders

Team leader on a redesign effort to increase the interactivity of a communication system
for emergency and everyday situations

Antenna Engineering Lab Assignment

Part of a team that redeveloped a lab to instruct students on how to use an anechoic
chamber for EE 438, Antenna Engineering

Professional Experience

April 2012 –   **Electrical Engineering Design Coop (Three Semesters)**
August 2013   *Lutron Electronics Co., Inc., Coopersburg, PA*
                    ○   Created and qualified an antenna for a Lutron product: the Radio
                    Shadow Sensor

- Qualified, configured and developed two radio ICs
- Worked as a lead electrical engineer in Aesthetics, Cognition and Ergonomics department on new product development
- Worked with supply chain and created a lifetime qualification plan to find less expensive, better parts for a cost reduction effort

January 2011 – Present	**Engineering Design Teaching Assistant**
	SEDTAPP, University Park, PA

- Guide engineering students through SolidWorks' uses
- Develop students understanding of design concepts

July 2006 – September 2007	**Research Assistant at Biology Lab**
	University of Pennsylvania, Philadelphia, PA

- Performed surgery to expose cochlear nerve in baby chicken
- Used a microelectrode probe to perform neural coding on the chicken